

REPORT DOCUMENTATION PAGE

Form Approved
OMB No. 0704-0188

Public reporting burden for this collection of information is estimated to average 1 hour per response, including the time for reviewing instructions, searching existing data sources, gathering and maintaining the data needed, and completing and reviewing this collection of information. Send comments regarding this burden estimate or any other aspect of this collection of information, including suggestions for reducing this burden to Department of Defense, Washington Headquarters Services, Directorate for Information Operations and Reports (0704-0188), 1215 Jefferson Davis Highway, Suite 1204, Arlington, VA 22202-4302. Respondents should be aware that notwithstanding any other provision of law, no person shall be subject to any penalty for failing to comply with a collection of information if it does not display a currently valid OMB control number. PLEASE DO NOT RETURN YOUR FORM TO THE ABOVE ADDRESS.

1. REPORT DATE (DD-MM-YYYY)	2. REPORT TYPE Technical Paper	3. DATES COVERED (From - To)
-----------------------------	-----------------------------------	------------------------------

4. TITLE AND SUBTITLE	5a. CONTRACT NUMBER
	5b. GRANT NUMBER
	5c. PROGRAM ELEMENT NUMBER

Please see attached

6. AUTHOR(S)	5d. PROJECT NUMBER 2308
	5e. TASK NUMBER M13C
	5f. WORK UNIT NUMBER 346057

7. PERFORMING ORGANIZATION NAME(S) AND ADDRESS(ES) ERC	8. PERFORMING ORGANIZATION REPORT
---	-----------------------------------

9. SPONSORING / MONITORING AGENCY NAME(S) AND ADDRESS(ES) Air Force Research Laboratory (AFMC) AFRL/PRS 5 Pollux Drive Edwards AFB CA 93524-7048	10. SPONSOR/MONITOR'S ACRONYM(S)
	11. SPONSOR/MONITOR'S NUMBER(S) Please see attached

12. DISTRIBUTION / AVAILABILITY STATEMENT

Approved for public release; distribution unlimited.

13. SUPPLEMENTARY NOTES

14. ABSTRACT

20030205 298

15. SUBJECT TERMS

16. SECURITY CLASSIFICATION OF:			17. LIMITATION OF ABSTRACT A	18. NUMBER OF PAGES	19a. NAME OF RESPONSIBLE PERSON Leilani Richardson
a. REPORT Unclassified	b. ABSTRACT Unclassified	c. THIS PAGE Unclassified			19b. TELEPHONE NUMBER (include area code) (661) 275-5015

MEMORANDUM FOR PRS (In-House Contractor Publication)

FROM: PROI (STINFO)

24 January 2002

SUBJECT: Authorization for Release of Technical Information, Control Number: **AFRL-PR-ED-TP-2002-013**
Bruce Chehroudi (ERC); Doug Talley (PRSA), "Preliminary Visualizations of Acoustic Waves
Interacting With Subcritical and Supercritical Cryogenic Jets"

15th Liquid Atomization & Spray Systems

(Statement A)

(Madison, WI, May 2002) (Deadline: 01 March 2002)

1. This request has been reviewed by the Foreign Disclosure Office for: a.) appropriateness of distribution statement, b.) military/national critical technology, c.) export controls or distribution restrictions, d.) appropriateness for release to a foreign nation, and e.) technical sensitivity and/or economic sensitivity.

Comments: _____

Signature _____ Date _____

2. This request has been reviewed by the Public Affairs Office for: a.) appropriateness for public release and/or b) possible higher headquarters review.

Comments: _____

Signature _____ Date _____

3. This request has been reviewed by the STINFO for: a.) changes if approved as amended, b) appropriateness of references, if applicable; and c.) format and completion of meeting clearance form if required

Comments: _____

Signature _____ Date _____

4. This request has been reviewed by PR for: a.) technical accuracy, b.) appropriateness for audience, c.) appropriateness of distribution statement, d.) technical sensitivity and economic sensitivity, e.) military/national critical technology, and f.) data rights and patentability

Comments: _____

APPROVED/APPROVED AS AMENDED/DISAPPROVED

PHILIP A. KESSEL Date
Technical Advisor
Space and Missile Propulsion Division

Preliminary Visualizations of Acoustic Waves Interacting With Subcritical and Supercritical Cryogenic Jets

Bruce Chehroudi
Engineering Research Corporation, Inc.
10 E. Saturn Boulevard
Edwards AFB, CA 93524-7680

Doug Talley*
Air Force Research Laboratory, AFRL/PRSA
10 E. Saturn Boulevard
Edwards AFB, CA 93524-7660

Abstract

The effect of large amplitude acoustic waves on subcritical and supercritical cryogenic jets was studied. A general trend was observed that acoustic waves cause the time averaged cross section of the jet to flatten in a direction where the minor axis becomes aligned with the direction of propagation of the waves. It was also found that the presence of acoustic waves shortened the breakup length of the jets compared with non-acoustically forced jets. The above trend was observed with decreasing magnitude as pressure increases from subcritical to supercritical pressures, until the trend became nearly indiscernible at the highest supercritical pressure evaluated. An increase in the mass flow rate of the jet also tended to decrease the magnitude of the trends observed.

Introduction

In a wide range of propulsion and energy conversion applications, high combustion chamber operating pressures tend to lead to performance and/or efficiency benefits. In some cases, chamber pressures have become high enough to exceed the thermodynamic critical pressure of one or more of the injected fluids. An example of relevance to the present study is the Space Shuttle Main Engine (SSME), fueled by liquid hydrogen and liquid oxygen. The main combustion chamber pressure in the SSME is about 22.3 MPa, or about four times the critical pressure of 5.043 MPa for oxygen. The initial temperature of the oxygen is initially below its critical temperature of 154.58 K, and then it undergoes a transition to a supercritical temperature as the oxygen is burned, in a so-called "transcritical" process. The injection behavior of cryogenic jets at rocket-like pressures has been the subject continuing study at the Air Force Research Laboratory (AFRL).

The AFRL study was initiated because at high enough pressures, injection and combustion processes are expected to become very different than conventional spray combustion processes. For example, the distinct difference between the gas and liquid phases disappears when either the pressure exceeds the critical pressure or the temperature exceeds the critical temperature. Near the critical point, the surface tension and enthalpy of vaporization vanish. Large variations in the density, thermal conductivity, and mass diffusivity also occur. For multi-component fluids, the solubility of the gas phase in the liquid phase increases as pressure approaches the critical pressure, and mixture effects need to be taken into account in calculating the critical properties. More information about the thermofluid behavior of substances under such conditions may be found in references [1-9].

Most recently, a study of the interaction of acoustic waves with isolated cryogenic jets as a function of pressure has been initiated. The motivation is to learn more about the mechanisms leading to combustion instabilities in high pressure liquid rocket engines. Combustion instabilities can cause engine damage within a fraction of a second, and have been known to produce pressure fluctuations reaching 100% of chamber pressure. They have always been one of the most complex and difficult to control phenomena in liquid rocket engines. In one mode known as "chugging," large amplitude pressure fluctuations are produced at relatively low frequencies (less than several hundred Hertz) due to coupling with feed line and structural modes of the engine. Chugging is responsive to system-type analysis. Another mode of instability known as "screaming" is characterized by high amplitudes and much higher frequencies, reaching several thousands of Hertz. Screaming can lead to local burnout of the combustion chamber walls and injector plates, due to extremely large heat-transfer rates brought about by the high frequency pressure and gas velocity fluctuations (see Harje and Reardon [10]).

Although numerous reports are available in the literature on most aspects of combustion instability, the interaction of acoustic waves with cryogenic jets at pressures approaching and exceeding the critical pressure appears never to have been systematically studied. The work reported here is our initial attempt to document such behavior. A more detailed description of the present work may be found in Chehroudi, et. al. [11]. Related relevant work by other researchers may be found in refs. [12-15], although the latter work did not address supercritical effects.

* Corresponding author

DISTRIBUTION STATEMENT A
Approved for Public Release
Distribution Unlimited

Experimental Setup

Nitrogen was used to simulate oxygen in the present study. Liquid nitrogen jets having a critical pressure of 3.39 MPa and a critical temperature of 126.2 K were injected into room temperature gaseous nitrogen at various chamber pressures. A schematic diagram of the experiment is shown in Fig. 1. Liquid nitrogen at atmospheric pressure was used to chill the high pressure nitrogen passing through a cryogenic heat exchanger just prior to injection to an initial temperature of between 99 - 110 K. This allowed the nitrogen to be measured and regulated by conventional room temperature flow meters and precision micrometer valves. Back-illumination of the jet was accomplished with diffuse light flashes of 0.8 μ s duration. A model K2 Infinity long distance microscope was used with a high resolution 1280 x 1024 CCD camera by the Cooke Corporation to form images of the injected jets. The jet was injected through a sharp-edged stainless steel tube with a length of 50 mm and inner and outer diameters of 0.254 mm and 1.59 mm, respectively. The resulting length-to-diameter ratio of 200 was sufficient to ensure fully developed turbulent pipe flow at the exit plane. The Reynolds number in these studies ranged from 14,000 to 80,000. The rig was fully instrumented to measure pressure, temperature, and the mass flow rate of the injected fluid. A piezo-siren specially designed by Hersh Acoustical Engineering (Westlake Village, CA) produced large amplitude acoustic waves at chamber pressures up to 13.4 MPa. The piezo-siren was enclosed in a suitable pressure housing, and acoustic waves were introduced into the chamber through a circular-to-rectangular transition coupling which focused the waves along the length of the jet and perpendicular to its axis.

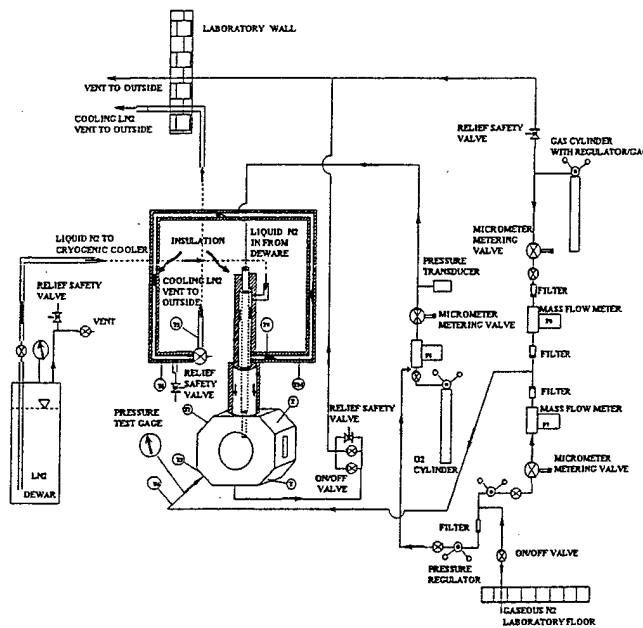


Figure 1. Schematic diagram of experimental setup for sub- to supercritical jet injection

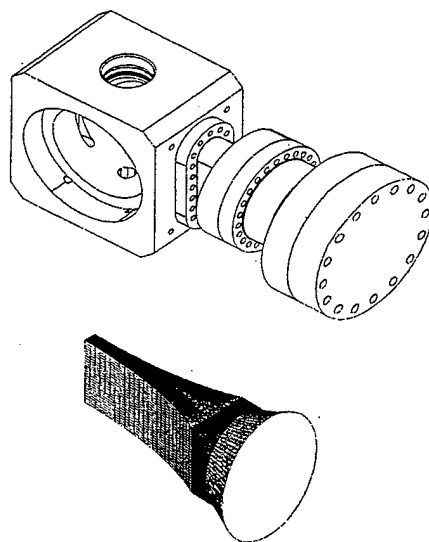


Figure 2. Top: coupling of the acoustic driver (piezo-siren) with the high-pressure chamber. Bottom: the design of the circular-to-rectangular channel to guide the waves into the chamber.

The pressure housing and the circular-to-rectangular transition geometry are illustrated in Fig. 2. A model 601B1 Kistler piezoelectric-type pressure transducer was used to measure the acoustic pressure variations inside the chamber at various locations very near the jet location.

Experimental Results

The piezo-siren was found to produce the largest acoustic amplitudes at two frequencies of approximately 2700 Hz and 4800 Hz when coupled to the chamber. The sound pressure level (SPL) was measured to range between 161 db to 171 db at these frequencies. Considering that the speed of the sound was about 357 m/s in the chamber, these frequencies correspond to acoustic wavelengths of about 13.1 cm and 7.4 cm. Both wavelengths were therefore much larger than the .254 mm initial diameter of the jets. During the initial investigation, it was found that a minimum oscillation amplitude threshold was required to cause a detectable interaction. When a rapid transition was made from below to above this minimum value, a strong and transitory effect was observed, characterized by the eruption of many drops and ligaments from the surface of the jet, combined with amplification of the surface wave instabilities.

Preliminary observations of the interaction of the acoustic waves with the nitrogen jets following the initial transitory period are presented in Figs. 3 and 4. No qualitative difference between the 2700 Hz and 4800 Hz case has yet been observed. Consequently, only the 4800 Hz case is shown in Figs. 3 and 4. The acoustic waves travel from left to right in Fig. 3, and they travel perpendicular to and out of the page in Fig. 4. Each figure shows three

image pairs, with each pair consisting of an image of a jet with the acoustics off, and an image of the same jet with the acoustics on. The top left image pair in each figure was taken at a subcritical pressure of 1.46 MPa, or a reduced pressure of 0.43. The bottom left image pair was taken at a near-critical pressure of 2.48 MPa, or a reduced pressure of 0.73. The top right image pair was taken at a supercritical pressure of 4.86 MPa, or a reduced pressure of 1.43. The jet flow rate was fixed at 150 mg/s for all cases. Up to 10 images were taken at each axial position, and a representative image was chosen to be displayed in Figs. 3 and 4. These images were taken in random phase to the acoustic waves. Each composite jet image consists of a representative mosaic of several images taken from the same run but at different times and jet axial locations.

Space allows only an indication of the broad trends represented by Figs. 3 and 4. A more detailed discussion and a more complete set of figures may be found in ref. [11].

Examination of the subcritical case in Fig. 3 reveals that the acoustic waves cause a constriction of the jet in the acoustic propagation direction near the injector exit, followed by the acceleration of the atomization process further downstream. The acceleration causes a relative broadening of the jet downstream compared with the non-acoustic case. However, Fig. 4 shows a much greater rate of broadening of the subcritical jet perpendicular to the direction of propagation. The net result is a time-averaged elliptical cross section having a minor axis aligned with the direction of propagation. Fig. 4 also shows that the breakup length of the jet is shortened by the presence of the acoustic waves.

Examination of the near-critical case in Figs. 3 and 4 shows the same trends as the subcritical case. However, the magnitude of the trends appears to be slightly reduced. As pressure is further increased above the critical pressure, the reduction in magnitude continues, but at a greater rate than at subcritical pressures. By the time the supercritical case in Figs. 3 and 4 is reached, the magnitudes have reduced to such an extent that the trends are nearly indiscernible. It would appear that the sensitivity of the jets to the presence of acoustic waves is reduced as pressure increases. This observation gives rise to the possibility that a supercritical state may couple relatively more poorly with combustion instabilities.

The effect of the mass flow rate of the jets was also examined. It was found that the impact of the acoustic waves on the jet was reduced as jet inertia forces increased through an increase of flow rate. This finding is consistent with the findings of Buffum and Williams [12] for subcritical jets.

Summary and Conclusions

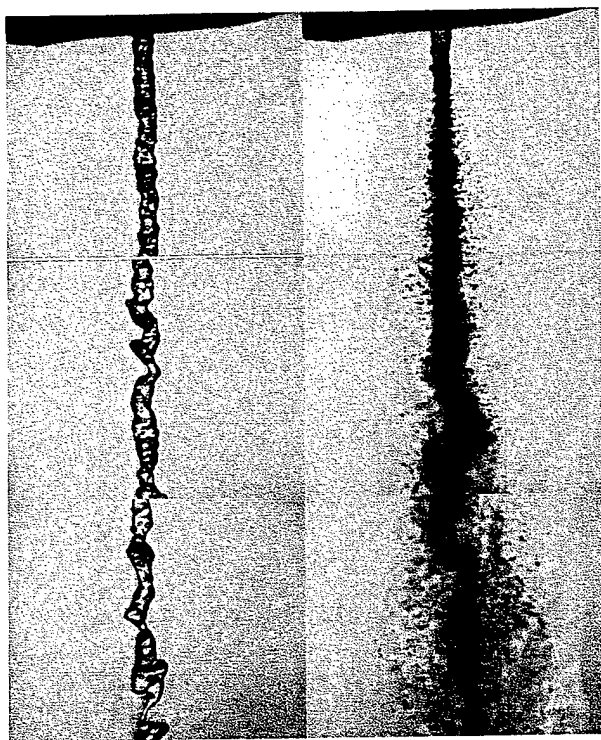
The effect of large amplitude acoustic waves on cryogenic nitrogen jets was studied, where the wavelength of the acoustic waves was much larger than the diameter

of the jets. The jets were injected initially at a subcritical temperature into room temperature gaseous nitrogen at various pressures ranging from subcritical to supercritical pressures. A general trend was observed that acoustic waves cause the time averaged cross section of the jet to flatten in a direction where the minor axis becomes aligned with the direction of propagation of the waves. It was also found that the presence of acoustic waves shortened the breakup length of the jets compared with non-acoustically forced jets. The above trend was observed with decreasing magnitude as pressure increases beyond the critical pressure, until the trend became nearly indiscernible at the highest supercritical pressure evaluated. An increase in the mass flow rate of the jet also tended to decrease the magnitude of the trends observed.

Mr. Mike Griggs and Mr. Earl Thomas are thanked for their valuable support. We also appreciate Mr. Kevin Bradley's contribution in part of the data acquisition and processing. Dr. Rich Cohn is thanked for kindly offering his expertise in image acquisition area. This work is sponsored by the Air Force Office of Scientific Research under Dr. Mitat Birkan, program manager.

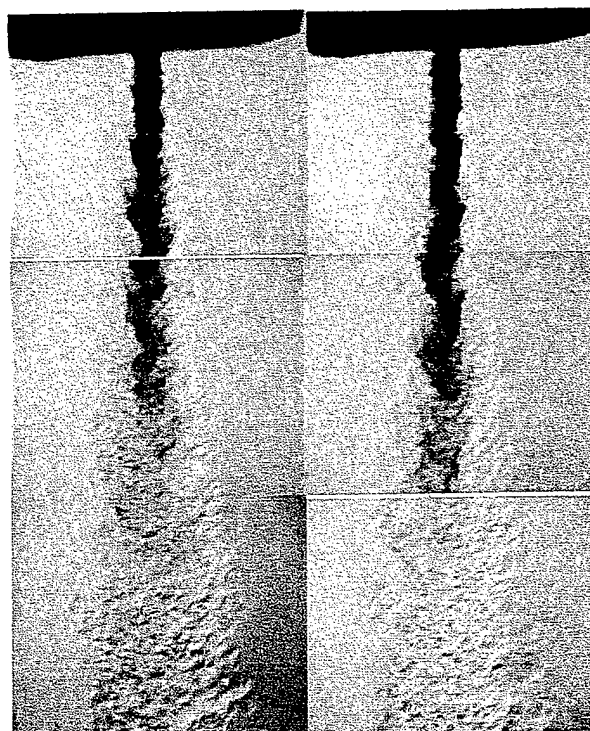
References

1. Bruno, T. J. and Ely, J. F., 1991. *Supercritical Fluid Technology*, CRC Press (1991).
2. Newman, J.A. and Brzustowski, *AIAA J.*, vol. 9, no. 8, pp. 1595-1602 (1971).
3. Chehroudi, *et al.*, *Phys. Fluids*, vol. 14, no. 2, (2002).
4. Chehroudi, *et al.*, *International J. of Heat and Fluid Flow*, to appear (2002).
5. Chehroudi, *et al.*, 36th Joint Propulsion Conference, paper AIAA-2000-3392 (2000).
6. Mayer, *et al.*, 32nd Joint Propulsion Conference & Exhibit, paper AIAA 96-2620 (1996).
7. Mayer, *et al.*, 34th Joint Propulsion Conference & Exhibit, paper AIAA 98-3685 (1998).
8. Oswald, M. and Schik, A, *Experiments in Fluids*, vol. 27, 497-506 (1999).
9. Oswald, *et al.*, 35th Joint Propulsion Conference and Exhibit, paper AIAA 99-2887 (1999).
10. Harrje, T. D. and Reardon, H. F., NASA SP-194 (1972).
11. Chehroudi, B., and Talley, D.G., 40th AIAA Aerospace Sciences Meeting and Exhibit, paper AIAA 2002-0342 (2002).
12. Buffum, F. G., and Williams, F. A., Proc. of the Heat Transfer and Fluid Mechanics Institute, P. A. Libby, D. B. Olfe, and C. W. Van Atta, eds, pp. 247-276 (1967).
13. Miesse, C.C., *Jet Propulsion*, 25, pp. 525-530, 1955.
14. Heidmann, M. F. and Groeneweg, J. F., NASA TN D-5339, July 1969.
15. Rockwell, D.O., *J. App. Mech.*, pp. 883-891, 1972.



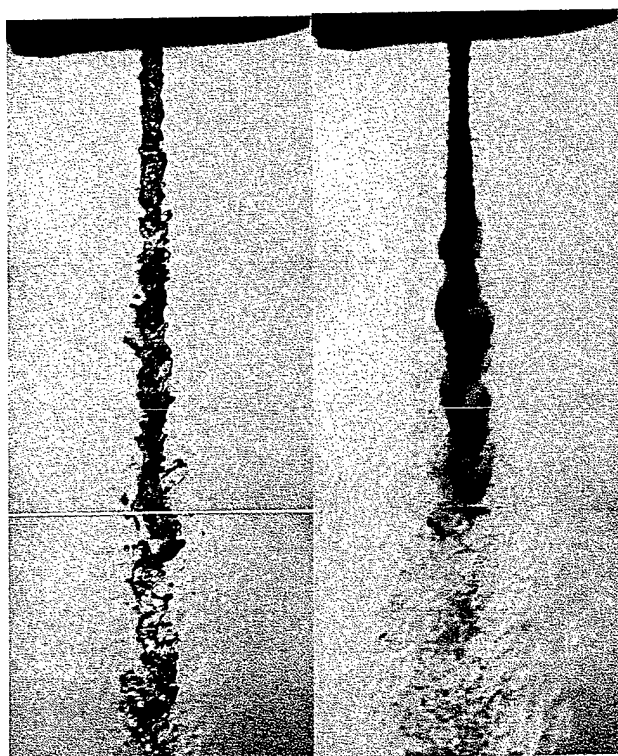
NORMAL
4800/1.46/150

ACOUSTIC ON
FRONT



NORMAL
4800/4.86/150

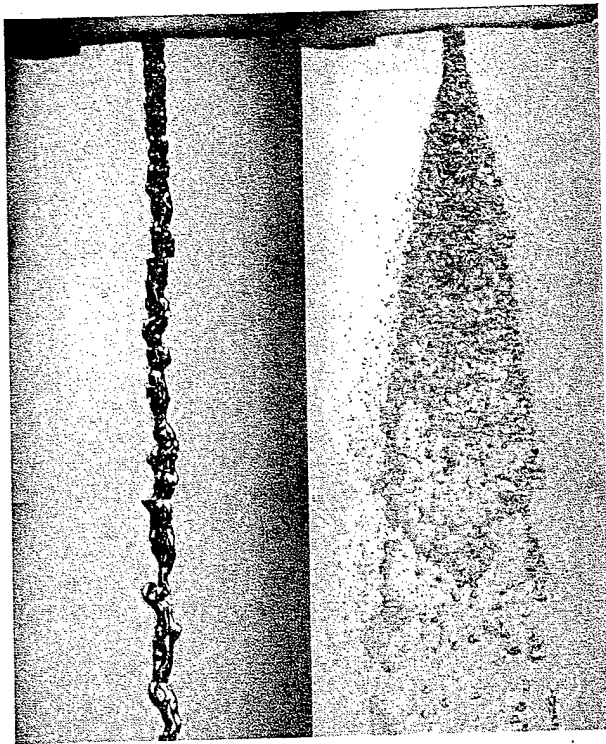
ACOUSTIC ON
FRONT



NORMAL
4900/2.48/150

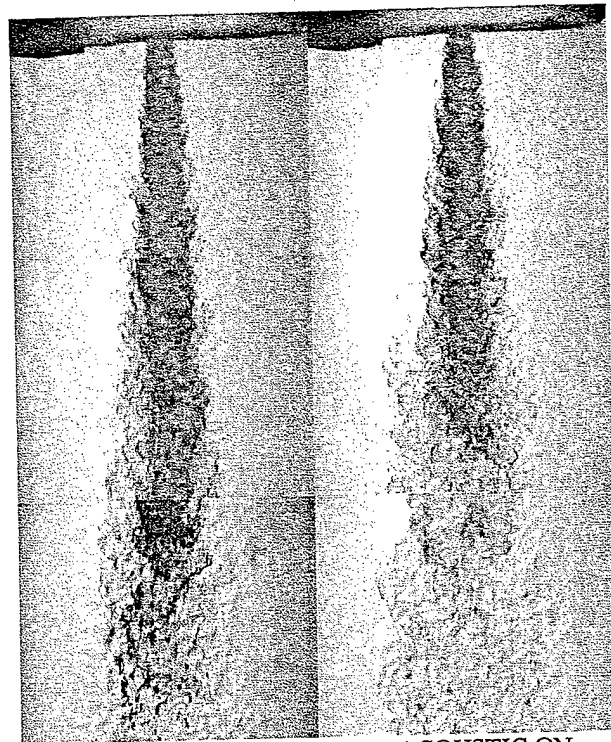
ACOUSTIC ON
FRONT

Figure 3. Images of the liquid nitrogen jet injected into the gaseous nitrogen chamber at subcritical (top left, $P = 1.46$ MPa), near-critical (bottom left, $P = 2.48$ MPa), and supercritical (top right, $P = 4.86$ MPa) chamber pressures. The injected flow rate was 150 mg/s. The acoustic waves traveled from left to right in these images. The acoustic wave frequency was set at 4800 Hz. Each composite jet image consists of mosaic of several images taken from the same run but at different times and jet axial locations.



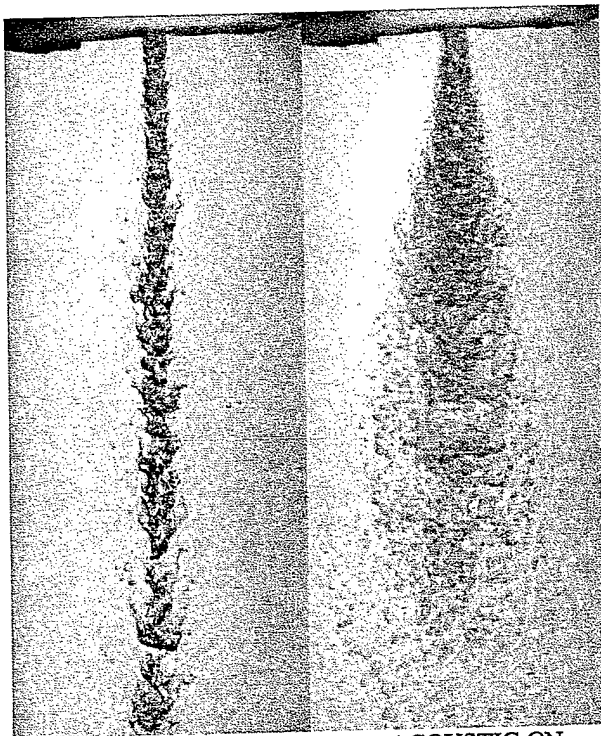
NORMAL
4800/1.46/150

ACOUSTIC ON
SIDE



NORMAL
4800/4.86/150

ACOUSTIC ON
SIDE



NORMAL
4800/2.48/150

ACOUSTIC ON
SIDE

Figure 4. Images of the liquid nitrogen jet injected into the gaseous nitrogen chamber at subcritical (top left, $P = 1.46$ MPa), near-critical (bottom left, $P = 2.48$ MPa), and supercritical (top right, $P = 4.86$ MPa) chamber pressures. The injected flow rate was 150 mg/s. The acoustic waves traveled perpendicular and out from the page in these images. The acoustic wave frequency was set at 4800 Hz. Each composite jet image consists of mosaic of several images taken from the same run but at different times and jet axial locations.